

Ternary Complexes of Cu (II), Ni (II), Co (II) and La (III) Ions with 2-[(Pyridin-2-Ylmethylidene) Amino] Phenol and Heterocyclic Nitrogen Base

Omyma A.M. Ali^{1*}, Samir M. El-Medani², Doaa A. Nassar³

¹Chemistry Department, Faculty of Women for Arts, Science and Education, Ain Shams University, Cairo, Egypt.

²Chemistry Department, Faculty of Science, El-Faiyum University, El-Faiyum, Egypt

***Corresponding Author:** Omyma A. M. Ali, Chemistry Department, Faculty of Women, Ain Shams University, Cairo, Egypt

Abstract: A new ternary Schiff base transition metal complexes of general formula $[M(HL)(2-AP)Cl_2].H_2O$ where $M = Cu(II), Ni(II)$ and $Co(II)$ ions in addition to the complex $[La(HL)(2-AP)(NO_3)_2].NO_3$ have been prepared by template synthesis. The synthesized metal complexes were characterized using spectroscopic techniques. The molar conductivities of the complexes in DMF indicated non electrolytic behavior except $La(III)$ complex. IR spectra show that the Schiff base (HL) is coordinated to the metal ions in a tridentate manner with NNO donor sites of the pyridine-N, azomethine-N and phenolic-O, while 2-aminopyridine coordinated to the metal ions via its pyridine-N. The ligand (HL) and its mixed ligand complexes exhibited intraligand ($\pi-\pi^*$) fluorescence and can potentially serve as photoactive materials. The catalytic activity of the complexes towards hydrogen peroxide decomposition reaction was investigated. Both the ligand (HL) and mixed ligand complexes have been screened for antibacterial activities.

Keywords: 2-Aminopyridine; Catalytic Activity; Fluorescence; Schiff Base.

1. INTRODUCTION

Schiff bases are one of the most prevalent and important of the mixed donor systems in the field of coordination chemistry. 2-Aminopyridines also serve as useful chelating ligands in a variety of inorganic and organometallic applications [1,2]. Amino pyridines and their derivatives in most cases act as monodentate ligands which coordinate the metal ions through the nitrogen of the ring [3,4]. Also, amino pyridines have been proposed as drugs for the treatment of many diseases such as myocardial infarction as antithrombus agents and diarrhea as antimicrobial agents [5,6]. Moreover, amino pyridines are commonly present in synthetic and natural products [7]. They form repeated moiety in many large molecules with interesting photophysical, electrochemical and catalytic applications [8]. The complexes with different types of heterocyclic such as amines, imines, oxazole, imidazole and ligands containing pyridine play an important role in biology and medicine areas. These ligands are often used in medicine, because of their pharmacological properties such as antibacterial activity [9,10]. On the other hand, complexes of Schiff base ligands derived from 2-pyridinecarboxaldehyde derivatives with some transition metals such as $Cu(II)$, $Co(II)$, $Cd(II)$ and $Zn(II)$ show significant biological activity [11,12]. Moreover, luminescent compounds are attracting much current research interest because of their many applications including emitting materials for organic light emitting diodes, light harvesting materials for photocatalysis and fluorescent sensors for organic or inorganic analytes [13-17]. The decomposition of hydrogen peroxide has been used as a model reaction for the investigation of the catalytic activity of various metal complexes [18]. For example, the catalytic activity of copper (II) complex of chitosan derivative which derived from chitosan and 4, 6-diacetylresorcinol was investigated on hydrogen peroxide decomposition [19]. Also, the mixed ligand complex $[Fe(2-AP)(Ala)Cl_3]4H_2O$ (2-AP = 2-acetylpyridine, Ala = alanine) catalyzed the decomposition of H_2O_2 and O_2 was evolved [20]. Herein, we report the transition metal complexes of Schiff base derived from the condensation of 2-pyridinecarboxaldehyde with 2-aminophenol. The ternary complexes were obtained by reaction with 2-aminopyridine. The structural features of these complexes were examined by analytical and spectral techniques.

2. EXPERIMENTAL

2.1. Materials and Reagents

2-pyridinecarboxaldehyde, 2-aminophenol and 2-aminopyridine were supplied by Aldrich. All metal salts used in this investigation $\text{CuCl}_2 \cdot 2\text{H}_2\text{O}$, $\text{NiCl}_2 \cdot 6\text{H}_2\text{O}$, $\text{CoCl}_2 \cdot 6\text{H}_2\text{O}$ and $\text{La}(\text{NO}_3)_3 \cdot 6\text{H}_2\text{O}$ were provided by Aldrich Chemicals. All solvents were of analytical grade and were purified by distillation before use.

2.2. Instruments

Infrared measurements using (KBr pellets) were carried out on a Unicam-Mattson 1000 FT-IR spectrometer and magnetic measurements of the complexes in the solid state (Gouy method) were recorded on a Sherwood magnetic susceptibility balance. ^1H NMR measurements were performed on a Varian-Mercury 300MHz spectrometer. Elemental analyses for carbon, hydrogen, and nitrogen (CHN) were performed on a Perkin-Elmer 2400 CHN elemental analyzer. Mass spectrometry measurement of the solid complex was carried out on a JEOL JMS- AX 500 spectrometer. Thermo gravimetric analyses (TG and DTG) were carried out under N_2 atmosphere with a heating rate of $10^\circ\text{C}/\text{min}$. using a Shimadzu DT-50 thermal analyzer. All conductivity measurements were performed in DMF (1×10^{-3} M) at 25°C , by using Jenway 4010 conductivity meter. The Photo luminescent properties of all compounds were studied using a Jenway 6270 Fluorimeter.

2.3. Synthesis of Schiff Base Hlligand

A methanolic solution of 2-pyridinecarboxaldehyde (0.9 g, 8.40 mmol) was added to a methanolic solution of 2-aminophenol (0.91 g, 8.40 mmol) and refluxed for ~11h and kept overnight. The resulting solution was then concentrated by evaporation and then the orange precipitate was formed. The precipitate formed was filtered and recrystallized from hot methanol to pure compound.

2.4. Synthesis of Mononuclear Mixed-Ligand Complexes

To an ethanolic solution of the metal salt (Cu(II), Ni(II), Co(II) and La(III)) a mixture of HL and 2-aminopyridine (2-AP) in a mixed solvent of DMF-THF (1:2) were added slowly. The metal-ligand molar ratio was (1:1:1). The reaction mixtures were refluxed for 5-7 h. The solid materials were filtered off and washed with ethanol and petroleum ether. The synthesized complex was dried at room temperature. Table 1 gives the elemental analysis and physical data for the complexes.

2.5. Catalytic Activity

The catalytic activity of the complexes has been evaluated by recording the rate of decomposition of hydrogen peroxide of known molarity prepared. The metal complex (4.1×10^{-3} - 8.2×10^{-3} mmol) was mixed with 50 ml of H_2O_2 (0.15 N) in a flask under constant stirring at room temperature. Then, the extent of hydrogen peroxide decomposed at different intervals of time (each 30 min; from 0 to 4.5 h) was estimated by titrating 5 ml aliquots of reaction mixture with 0.01 M KMnO_4 in the presence of 0.01 M H_2SO_4 . The difference in titer values of the KMnO_4 solution before and after the catalyzed decomposition was recorded.

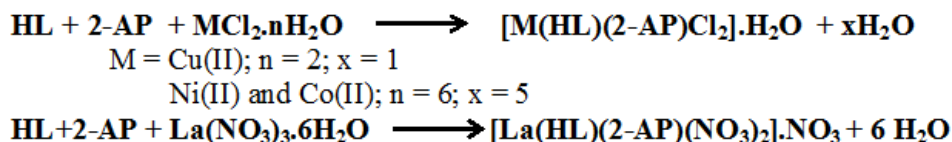
2.6. Antibacterial Activity

The in vitro antimicrobial activities of the free ligand and its complexes were tested against the bacteria: Staphylococcus aureus (gram +ve) and Escherichia coli (gram -ve) in Mueller Hinton-Agar medium. The standard disc diffusion method was followed to determine the antibacterial activity of the synthesized compounds. The well (8 mm diameter) was then filled with the test solution and the plates were inoculated at 37°C for 48 h. During this period, the growth of the inoculated microorganisms was affected and then the inhibition zones developed on the plates were measured. The effectiveness of an antibacterial agent was assessed by measuring the zones of inhibition around the well. The diameter of the zone is measured to the nearest millimeter (mm). The antibacterial activity of each compound was compared with that of standard antibiotics such as Tetracycline. DMSO was used as a control under the same conditions for each organism and no activity was found. The activity results were calculated as a mean of triplicates.

3. RESULTS AND DISCUSSION

The reaction of Schiff-base ligand (HL) with Cu(II), Ni(II), Co(II) and La(III) ions in the presence of 2-aminopyridine produce the ternary complexes having the molecular formula as shown in Table

1.The synthesized mixed ligand complexes were found to be air stable, moisture free and soluble only in DMF and DMSO. The course of the reactions may be as follows:



3.1. IR Spectra

The IR spectral data of Schiff base [HL] and ternary complexes are presented in Table 2. The infrared spectrum of HL exhibited vibrational bands at 3387 and 1247 cm^{-1} due to $\nu(\text{OH})$ and $\nu(\text{C-O})$ bonds. In addition, the IR spectrum of the HL displayed $\nu(\text{C=N})$ at 1630 and 1590 cm^{-1} for both azomethine and pyridyl moieties, respectively. The IR spectra of the Cu(II), Ni(II), Co(II) and La(III) ternary complexes showed characteristic bands due to OH, C-O and C=N function groups with the appropriate shifts due to complex formation. In addition, the IR-spectra of the ternary complexes containing 2-aminopyridine as a secondary ligand showed that the band characterizing the stretching vibration for NH_2 group (occurring at 3447 and 3307 cm^{-1}) overlapped with OH group. The two bands at 1501 cm^{-1} and 630 cm^{-1} characteristic to $\nu(\text{C=N})$ and $\delta(\text{py})$ for 2-aminopyridine shifted in the complexes indicating the involvement of pyridine ring nitrogen in coordination and so, 2-aminopyridine acts as a neutral monodentate ligand [21]. Interestingly, the in-plane ring deformation band of py in HL ligand is found at 625 cm^{-1} . On complexation, this band of py shifted to higher frequencies, suggesting the coordination of pyridyl nitrogen to metal. Four intense bands in the spectrum of La(III) complex observed at 1445, 1034, 1311 and 818 cm^{-1} . The separation frequency of 134 cm^{-1} between 1445 (ν_s) and 1311 (ν_{as}) is consistent with the value reported in literature for the nitrate group coordinates in a bidentate manner [22,23]. In addition, there is a band at 1384 cm^{-1} in the spectrum of the La(III) complex indicates that the existence of free nitrate group in the ionization sphere [24]. The presence of non-ligand bands in the spectra of complexes in the region 545–550 cm^{-1} and 410–451 cm^{-1} were assigned to $\nu(\text{M-O})$ and $\nu(\text{M-N})$ stretching vibrations, respectively [25].

3.2. ^1H NMR Spectra

Proton NMR spectrum of HL was compared with the diamagnetic mixed ligand La(III) complex in deuterated DMSO using TMS (tetramethylsilane) as internal standard. The ^1H NMR spectrum of the free Schiff base ligand HL showed signal at 10.09 ppm attributed to the OH proton. The ^1H NMR spectrum of La(III) complex displayed a signal at 10.18 ppm indicating the coordination of HL ligand to lanthanum atom through the hydroxyl group without deprotonation. The shifting of azomethine ($-\text{CH=N}-$) group in free ligand from 8.59 ppm to 8.62 ppm in the La(III) complex indicates that the azomethine group is involved in the complexation. The chemical shifts of the different types of protons in the ^1H NMR spectra of the HL ligand and La(III) complex are listed in Table 3.

3.3. Mass Spectra Analysis

The mass spectrum of the ligand HL displayed the parent molecular ions $[\text{M}]^+$ at $m/z = 198$, and important fragments at 52 (35%) $[\text{C}_4\text{H}_4]^+$, 65 (40%) $[\text{C}_4\text{H}_3\text{N}]^+$, 79 (71%) $[\text{C}_5\text{H}_5\text{N}]^+$ and 93 (19%) $[\text{C}_6\text{H}_5\text{O}]^+$.

The mass spectrum of $[\text{Cu}(\text{HL})(2\text{-AP})\text{Cl}_2] \cdot \text{H}_2\text{O}$ complex (Fig. 1) gave molecular ion peak at 445 (F.Wt. = 444.8). The spectrum exhibits a peak at 427 (Calc. 426.7) corresponding to the removal of hydrated water molecule. This fragment ion underwent fragmentation with loss of the two chlorine atoms gave a peak at 357.00 (Calc. 355.8). Further fragmentation with loss of 2-AP ligand gave a peak at 261.00 (Calc. 261.76).

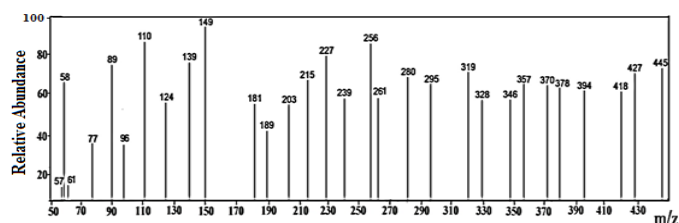


Figure 1. The mass spectrum of $[\text{Cu}(\text{HL})(2\text{-AP})\text{Cl}_2] \cdot \text{H}_2\text{O}$ complex

The Mass spectrum of [Co (HL) (2-AP) Cl₂].H₂O complex (Fig. 2) observed a molecular ion peak at 440 (F.Wt = 440.1). The existence of both primary and secondary ligands are indicated by the peaks at 197 and 94 (Calc.198.2 and 94.1), respectively. The removal of hydrated water molecule indicated by the peak at 421 (Calc.422.2). This fragment ion underwent fragmentation with the loss of the water molecule and two chlorine atoms gave a peak at 353 (351.27).

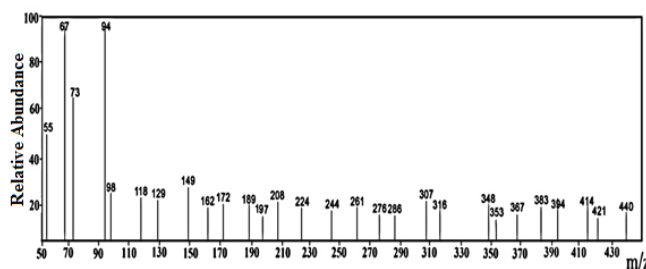


Figure2. The mass spectrum of [Co(HL)(2-AP)Cl₂].H₂O complex.

The Mass spectrum of [Ni(HL)(2-AP)Cl₂].H₂O complex (Fig. 3) exhibited a molecular ion peak at 440 (Calc.439.9). The existence of both primary and secondary ligands are indicated by the peaks at 199 and 94 (Calc.198.2 and 94.1), respectively. The spectrum exhibits a peak at 421 (Calc.421.9) corresponding to the removal of hydrated water molecule. This fragment ion underwent fragmentation with the loss of the water molecule and two chlorine atoms gave a peak at 353 (351.27).

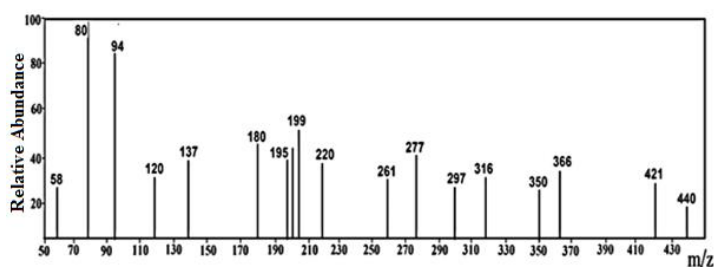


Figure3. The mass spectrum of [Ni(HL)(2-AP)Cl₂].H₂O complex.

3.4. Conductivity Measurements

The conductance measurements recorded for 10⁻³ M solutions of metal complexes in DMF are listed in Table (1). Cu (II), Ni (II) and Co (II) complexes are non-conducting having conductance values of 10-13 Ω⁻¹mol⁻¹cm² indicating their neutrality, so the chloride anion is situated inside the metal coordination sphere. The electrical conductance value of La(III) chelate is found to have molar conductance value of 87 ohm⁻¹mol⁻¹cm² indicating its electrolytic nature as 1:1 electrolyte [26]

3.5. Electronic Spectra and Magnetic Moment Values

The diffuse reflectance spectra of the HL and the mixed ligand complexes are listed in Table 4. HL showed three bands at 243, 278 and 307 unattributed to π-π*, n-π* and charge transfer transition, respectively. The Cu(II) complex showed a broad band at 608 nm assignable to ²E_g→²T_{2g} transition, which is characteristic of distorted octahedral configuration [27]. The measured value of the magnetic moment lies in the range reported for octahedral complexes (1.95 B.M.). The Ni(II) complex has magnetic moment value of 2.99 B.M., which correspond to two unpaired electrons about Ni(II) ion for six-coordinated octahedral geometry [28]. The electronic spectrum of Ni(II) complex displayed three bands in the solid reflectance spectrum at ν₁ (704nm: ³A_{2g}→³T_{2g}); ν₂ (606nm: ³A_{2g}→³T_{1g}(F)) and ν₃ (476nm: ³A_{2g}→³T_{1g}(P)) [29]. The diffuse reflectance spectrum of the Co(II) complex showed three bands at 473, 605 and 734 nm. The bands observed are assigned to the transition ⁴T_{1g}(F)→⁴T_{1g}(P) (ν₃), ⁴T_{1g}(F)→⁴A_{2g}(F) (ν₂) and ⁴T_{1g}(F)→²T_{2g}(F) (ν₁), respectively, suggesting the octahedral structure around Co(II) ion [30]. The magnetic moment value of Co(II) complex has been found to be 4.22 BM corresponding to three unpaired electrons within the range of high spin octahedral complex of Co(II) ion [31]. The diffuse reflectance spectrum of La (III) (d⁰) complex showed π-π* and n-π* bands at 244 and 278 nm, respectively. In addition, another bands displayed in the range 349-384 nm attributed to ligand to metal charge transfer. As expected for the diamagnetic La (III) (d⁰) configuration, ligand field band due to d-d electronic transitions is not expected [32].

3.6. Luminescence Spectral Study

The fluorescence properties of the Schiff base ligand (HL) and ternary complexes (Fig. 4) were recorded in DMSO at room temperature. The excitation spectrum of the HL ligand showed a maximum emission peak at 430nm when excited at 310nm. Generally, Schiff base systems exhibit fluorescence due to intraligand $\pi \rightarrow \pi^*$ transitions. The fluorescent data are summarized in Table 5. The excitation spectra of Cu(II), Ni(II), Co(II) and La(III) complexes exhibited a strong blue fluorescence emission band in the range 359-364nm when excited at 304-330 nm. Significant differences in the positions of emission maximum of Schiff base and its complexes establish the coordination of the metal ion to the ligand. The fluorescence spectral results reveal that the fluorescence emission intensity of Schiff base increases dramatically on complex formation with transition metal ions. Enhancement of fluorescence through complexation is much interesting as it opens up the opportunity for photochemical applications of these complexes [33]. In general, all the synthesized compounds can serve as potential photoactive materials, as indicated from their characteristic fluorescence properties.

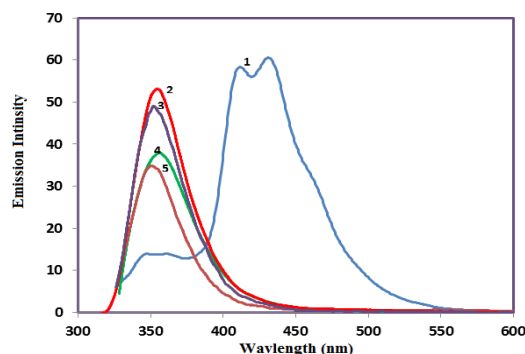
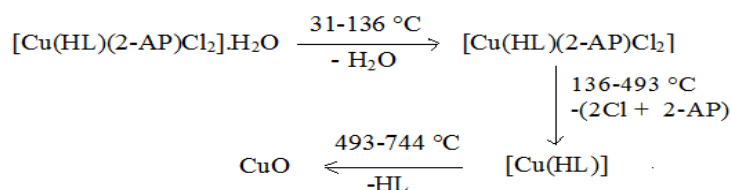


Figure 4. Emission spectra of: (1) HL; (2) $[Cu(HL)(2-AP)Cl_2] \cdot H_2O$; (3) $[Ni(HL)(2-AP)Cl_2] \cdot H_2O$; (4) $[Co(HL)(2-AP)Cl_2] \cdot H_2O$; (5) $[La(HL)(2-AP)(NO_3)_2] \cdot NO_3$

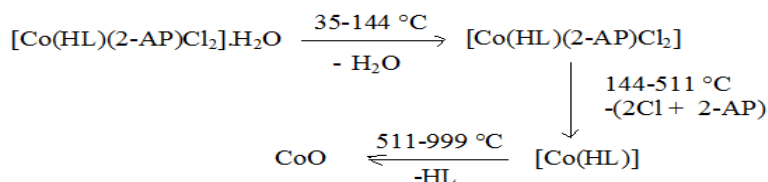
3.7. Thermal Analysis (TGA And Drtga)

The thermal studies of mixed ligand complexes were carried out using the thermo gravimetric technique (TG) and differential thermo gravimetric (DTG). Table 6 gives the detailed thermal decomposition data for complexes.

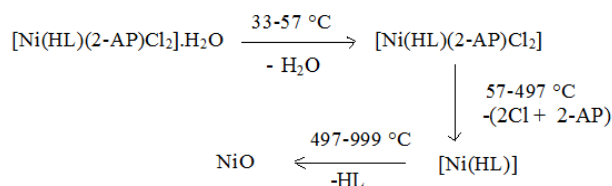
The TG/DTG curves of $[Cu(HL)(2-AP)Cl_2] \cdot H_2O$ complex showed three decomposition steps in the range of 31-136°C, 136-493°C and 493-744°C. The first decomposition step due to the elimination of H_2O with weight loss of 4.16 % (Calc. 4.04 %). The second decomposition step assigned to the loss of the two chlorine atoms and 2-AP with weight loss of 37.01 % (Calc. 37.09 %). The third decomposition step could be attributed to the loss of the (HL) ligand with weight loss of 41.06 % (Calc. 40.96 %) leaving CuO as residue.



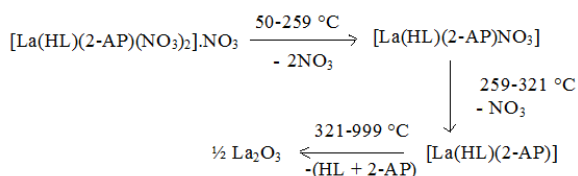
The TGA curves of $[Co(HL)(2-AP)Cl_2] \cdot H_2O$ complex showed three decomposition peaks. The first decomposition step occurs in the range 35-144°C with mass loss observed is 4.1 % (Calc. 4.28%) which attributed to the loss of the H_2O molecule. The second step of decomposition takes place in the range 144-511°C with mass loss 37.24% (Calc. 37.48%) which due to a loss of 2-AP and the two chlorine atoms. The third decomposition step occurs in the range 511-999°C with mass loss 40.79% (Calc. 41.39%) which corresponding to the loss of HL leaving CoO as residue.



The TG plot of $[\text{Ni}(\text{HL})(2\text{-AP})\text{Cl}_2]\cdot\text{H}_2\text{O}$ displayed three decomposition steps. The first step due to the release of the water molecule and the mass loss observed is 4.00% against the calculated loss of 4.08% and occurred in the range 33-57°C. The second step occurred in the range 57-497°C with a mass loss of 37.50% (Calc. 37.50 %) attributed to the loss of 2-AP and the two chlorine atoms. The third step occurs in the range 497-999°C with the mass loss of 42.29% (Calc. 41.39 %) which corresponding to a loss of HL leaving NiO as residue.



The TGA curves of $[\text{La}(\text{HL})(2\text{-AP})(\text{NO}_3)_2]\cdot\text{NO}_3$ complex showed three decomposition steps. The first decomposition step occurred in the range 50-259 °C with a weight loss of 20.15 % (Calc. 20.09 %). The percentage loss was consistent with the elimination of the two nitrate groups. The second decomposition stage occurred in the range 259-321 °C with a weight loss of 10.07 % (Calc. 10.04 %) could be attributed to the loss of the remaining nitrate group. The third decomposition step occurs in the 321-999°C range with a weight loss of 47.42 % (Calc. 47.34 %) corresponding to loss of the ligands leaving $\frac{1}{2}\text{La}_2\text{O}_3$ as residue.



The activation energy (E^*), enthalpy (H^*), entropy (S^*) and Gibbs free energy change of the decomposition (G^*) were evaluated graphically by employing the Coats-Redfern relation [34].

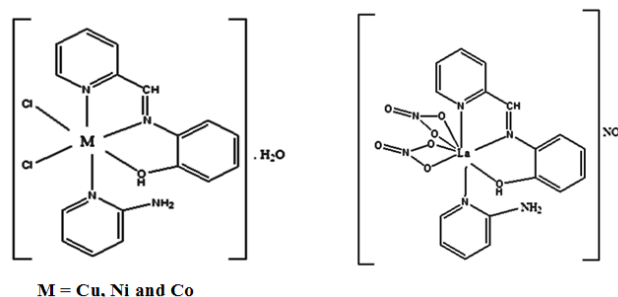
$$\log\left[\frac{\log(W_\infty / (W_\infty - W))}{T^2}\right] = \log\left[\frac{AR}{\phi E^*}\left(1 - \frac{2RT}{E^*}\right)\right] - \frac{E^*}{2.303RT} \quad (1)$$

Where W_∞ is the mass loss at the completion of the decomposition reaction, W is the mass loss up to temperature T , R is the gas constant and ϕ is the heating rate. Since $1 - 2RT/E^* \cong 1$, the plot of the left-hand side of equation (1) against $1/T$ would give a straight line. E^* was then calculated from the slope and the Arrhenius constant, A , was obtained from the intercept. The other kinetic parameters; the entropy of activation (S^*), enthalpy of activation (H^*) and the free energy change of activation (G^*) were calculated using the following equations:

$$H^* = E^* - RT; G^* = H^* - TS^* \text{ and } S^* = 2.303 R \log \frac{Ah}{kT}$$

Where, (k) and (h) are the Boltzman and Planck constants, respectively. The kinetic parameters are listed in Table 7. From the obtained results, it is apparent that G^* values of the complexes acquire highly positive magnitudes. The activation energies of decomposition were found to be in the range 28.5 - 693.1 KJmol^{-1} . The high value of the energy of activation of the complexes revealed the high stability of the investigated complexes due to their covalent character [35]. Additionally, the negative values of entropy indicate that the activated complex has more ordered systems than reactants [36].

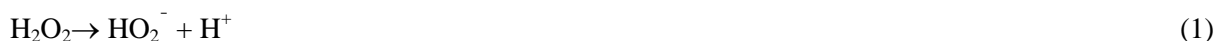
In the light of all results, the most reasonable structures of the ternary complexes are shown in Scheme 1.



Scheme1. The proposed structure of mixed ligand complexes

3.8. Catalytic Activity

The decomposition of hydrogen peroxide has been used as a model reaction for the investigation of the catalytic activity of various ternary complexes. The decomposition of H₂O₂ catalyzed by metal complexes has been monitored by titrating the undecomposed H₂O₂ with a standard KMnO₄ solution. Variables such as the time were found to have important roles in the decomposition of H₂O₂. The effect of time on decomposition of H₂O₂ at a constant concentration of H₂O₂ (0.15 N) and constant concentration of complexes (6.4x10⁻³-9.0x10⁻³ mmol⁻¹) at 25⁰C were studied (Tables8-11).The conditions of catalytic reactions for hydrogen peroxide decomposition were chosen according to the similar studies in the literature [37,38]. The results showed that the percentage of decomposition of hydrogen peroxide increased with the time (Fig. 5). It was observed that 4.5h is an adequate reaction time for decomposition of 42.5-72% of H₂O₂ catalyzed by complexes. In the absence of a complex, the percentage of decomposition of hydrogen peroxide occurred spontaneously is 20 % after 24 h. The mechanism of the catalytic reaction has been proposed in the literature [39] is given in formulas (1)–(3):



The M-L complex may interact with HO₂⁻ ions to form an intermediate complex.



A second molecule of H₂O₂ may then interact with the intermediate complex to form the following products.



Catalytic decomposition of H₂O₂ leads to the formation of intermediate radical species which can bind to the surfaces where H₂O₂ undergoes decomposition [40, 41]. The enhanced catalytic activity of the complex system may be explained on the basis of the formation of the above intermediate peroxy species. When a metal complex is bound to a support its motion is restricted. Reactions on such catalysts are expected to be more rapid than one on which the catalyst molecules are free [42].

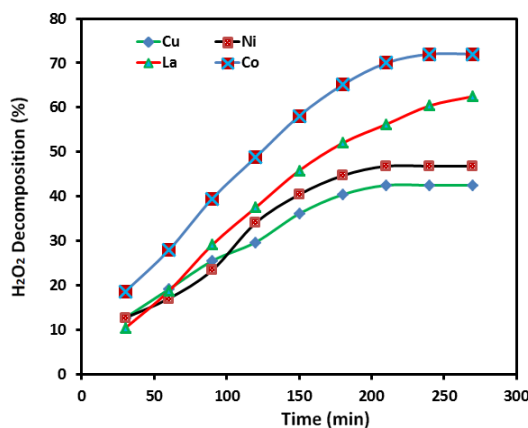


Figure5. Effect of reaction time on decomposition of H₂O₂ with [Cu(HL)(2-AP)Cl₂].H₂O, [Co(HL)(2-AP)Cl₂].H₂O, [Ni(HL)(2-AP)Cl₂].H₂O and [La(HL)(2-AP)(NO₃)₂].NO₃ complexes at 25 °C.

3.9. Antibacterial Activity

Antibacterial activity of Schiff base ligand and ternary complexes have been tested against one gram positive bacteria; *S. aureus* and also against one gram negative bacteria; *E.coli* microorganisms. The antibacterial activities obtained for the prepared compounds are listed in Table 12. All the investigated compounds showed a remarkable biological activity against bacteria (Fig. 6).The obtained results reflect that; (1) The ligand, Cu(II) and Co(II) complexes possessed moderate activity against *E. Coli.*; (2) Ni(II) and La(III) complexes showed lower activity than HL against *E. Coli.*; (3) All complexes showed higher activity than ligand against *S. aureus*. On chelation, the delocalization of π -electrons over the whole chelate ring will be increased which enhances the penetration of the complexes into lipid membranes and blocking the metal binding sites in the enzymes of microorganisms. Also, the tested complexes may disturb the respiration process of the cell and consequently block the synthesis of proteins leading to no further growth of the organisms [43]. The variation in the activity values of different compounds against different organisms depends on either the impermeability of the cells of the microbes or on the differences in ribosome of microbial cells [44].

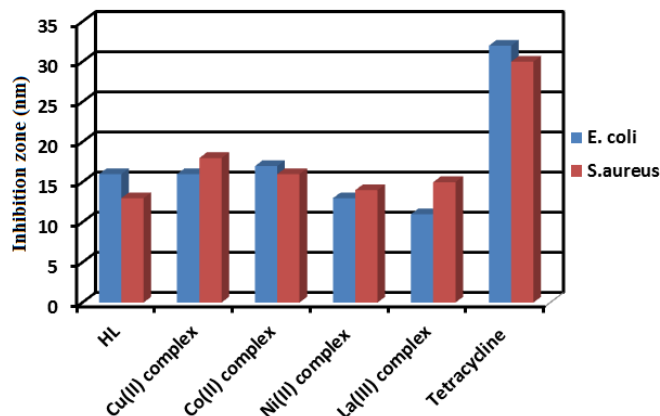


Figure6. Antibacterial activity of compounds under study.

Table1. Analytical and physical data of the Schiff base (HL) and mixed ligand complexes.

Compound	M.Wt.	Color (% yield)	Elemental analysis found (Calc.)			M.p. (°C)	A (Ω^{-1} mol^{-1} cm^2)
			C %	H %	N %		
$\text{C}_{12}\text{H}_{10}\text{N}_2\text{O}$	198.22	Dark Yellow (80)	72.11 (72.71)	5.21 (5.08)	14.22 (14.13)	220	-
$[\text{Cu}(\text{C}_{17}\text{H}_{16}\text{N}_4\text{O})\text{Cl}_2] \cdot \text{H}_2\text{O}$	444.80	Dark red (89)	45.92 (45.90)	4.08 (4.07)	12.59 (12.59)	>300	10
$[\text{Co}(\text{C}_{17}\text{H}_{16}\text{N}_4\text{O})\text{Cl}_2] \cdot \text{H}_2\text{O}$	440.19	Brick red (87)	45.42 (46.38)	3.96 (4.12)	13 (12.73)	>300	13
$[\text{Ni}(\text{C}_{17}\text{H}_{16}\text{N}_4\text{O})\text{Cl}_2] \cdot \text{H}_2\text{O}$	439.97	Crimson (85)	46.25 (46.40)	4.35 (4.12)	12.50 (12.73)	>300	12
$[\text{La}(\text{C}_{17}\text{H}_{16}\text{N}_4\text{O})\text{NO}_3)_2] \cdot \text{N O}_3$	617.26	Brown (70)	42.37 (33.08)	3.82 (2.61)	13.7 (15.88)	>300	87

Table2. IR data of the Schiff base (HL) and mixed ligand complexes (cm^{-1}).

Compound	IR (cm^{-1}) ^a						
	ν (OH) or ν (NH_2)	ν (C=N)	ν (C-O)	δ (py)	ν (M-O)	ν (M-N)	Other bands
HL	3387(b)	1630(w) 1590(s)	1247(m)	625(w)	—	—	—
$[\text{Cu}(\text{HL})(2\text{-AP})\text{Cl}_2] \cdot \text{H}_2\text{O}$	3321(b) 3403(b)	1661(m) 1626(s) 1567(m)	1261(m)	648(w) 636(w)	549(w)	450(w)	—
$[\text{Co}(\text{HL})(2\text{-AP})\text{Cl}_2] \cdot \text{H}_2\text{O}$	3314(b) 3380(b)	1663(s) 1631(m) 1593(m)	1275(s)	662(w) 650(w)	550(w)	451(w)	—
$[\text{Ni}(\text{HL})(2\text{-AP})\text{Cl}_2] \cdot \text{H}_2\text{O}$	3302(b)	1662(s) 1621(m) 1595(m)	1271(m)	650(w) 612(w)	545(w)	425(w)	—
$[\text{La}(\text{HL})(2\text{-AP})(\text{NO}_3)_2] \cdot \text{NO}_3$	3333(b)	1664(s) 1624(w) 1591(s)	1260(sh)	671(w) 638(w)	547(w)	410(w)	1445(s) 1034(w) 1311(m) 818(w)

^am, medium; s, strong; w, weak; sh, shoulder

Table3. ¹H NMR spectral data of the Schiff base HL and La(III) complex

Compound	Chemical shift, δ (ppm) ^a
HL	7.53-7.27 m (4H, aromatic), 8.39-7.92 m (4H, pyridine), 8.59 s (1H, HC=N), 10.09 s (1H, OH).
$[\text{La}(\text{HL})(2\text{-AP})(\text{NO}_3)_2] \cdot \text{NO}_3$	6.54-6.52 m (4H, aromatic), 7.93-7.45 m (4H, pyridine), 8.62 s (1H, HC=N), 10.18 s (1H, OH).

^a s, singlet; m, multiplet.

Table4. The diffuse reflectance data of the Schiff base (HL) and mixed ligand complexes

Compound	λ_{max} (nm)			
	$\pi-\pi^*$	$n-\pi^*$	Charge transfer	d-d transition
HL	243	278	307	-
[Cu(HL)(2-AP)Cl ₂].H ₂ O	255	280	353	608
[Co(HL)(2-AP)Cl ₂].H ₂ O	246	269	350, 384	473, 605, 734
[Ni(HL)(2-AP)Cl ₂].H ₂ O	244	269	349, 384	476, 606, 704
[La(HL)(2-AP)(NO ₃) ₂].NO ₃	244	278	349, 384	-

Table5. Fluorescence data of the Schiff base (HL) and mixed ligand complexes

Compound	$\lambda_{excitation}$	$\lambda_{emission}$
HL	310	349, 410, 430
[Cu(HL)(2-AP)Cl ₂].H ₂ O	304	359
[Co(HL)(2-AP)Cl ₂].H ₂ O	318	364
[Ni(HL)(2-AP)Cl ₂].H ₂ O	330	360
[La(HL)(2-AP)(NO ₃) ₂].NO ₃	318	360

Table6. Thermogravimetric data of mixed ligand complexes.

Complex	TG range (°C)	Mass loss %		Assignment	Metallic residue Calc. (found)
		Calc.	Found		
[Cu(HL)(2-AP)Cl ₂].H ₂ O	31-136	4.05	4.16	Loss of H ₂ O	CuO 17.88% (17.77%)
	136-493	37.11	37.01	Loss of 2Cl +2-AP	
	493-744	40.96	41.06		
[Co(HL)(2-AP)Cl ₂].H ₂ O	35-144	4.10	4.28	Loss of H ₂ O	CoO 17.03 % (17.69 %)
	144-511	37.48	37.24	Loss of 2Cl+2-AP	
	511-999	41.39	40.79	Loss of (HL)	
[[Ni(HL)(2-AP)Cl ₂].H ₂ O	33-57	4.09	4.00	Loss of H ₂ O	NiO 16.99 % (17.01 %)
	57-497	37.51	37.70	Loss of 2Cl +2AP	
	497-999	41.41	41.29	Loss of (HL)	
[La(HL)(2AP)(NO ₃) ₂].NO ₃	50-259	20.09	20.15	Loss of 2NO ₃	½ La ₂ O ₃ 26.40 % (26.52%)
	259-321	10.04	10.07	Loss of NO ₃	
	321-999	43.47	43.18	Loss of (2AP+HL)	

Table7. Thermodynamic data of the thermal decompositions steps of mixed ligand complexes

Complex	Decomposition range (°C)	E*/kJmol ⁻¹	A(S ⁻¹)	S*/K ⁻¹ Jmol ⁻¹	H*/kJmol ⁻¹	G*/kJmol ⁻¹
[Cu(HL)(2-AP)Cl ₂].H ₂ O	136-298	42.52	2.3x10 ³	-178.17	40.66	80.39
	466-715	68.13	3.8x10 ²	-202.56	62.29	204.44
[Co(HL)(2-AP)Cl ₂].H ₂ O	79-330	28.55	3.8x10 ¹	-214.47	26.09	89.30
	414-664	63.65	5.6x10 ²	-198.17	58.61	178.62
	709-801	374.19	2.3x10 ⁷	-379.80	367.70	663.39
	802-886	693.13	2.7x10 ²⁰	-628.00	686.02	120.99
[[Ni(HL)(2-AP)Cl ₂].H ₂ O	33-109	39.51	1.8x10 ⁵	-129.50	388.98	45.38
	113-347	42.86	1.2x10 ³	-183.29	41.04	81.09
	432-747	65.53	4.9x10 ²	-198.59	60.29	170.96
[La(HL)(2-AP)(NO ₃) ₂].NO ₃	92-249	30.89	1.89x10 ²	-199.22	28.98	74.76
	250-345	108.45	1.05x10 ⁹	-72.41	106.0	128.06
	385-543	150.47	4.4 x10 ⁹	-63.94	146.57	176.54

Table8. Effect of time on decomposition of H₂O₂ at constant concentration of H₂O₂ (0.15 N) and Cu(II) complex (7.6x10⁻³ mmol) at 25 °C.

	Time (Minutes)								
	30	60	90	120	150	180	210	240	270
Baseline KMnO ₄ (a)	4.7 mL	4.7 mL	4.7 mL	4.7 mL	4.7 mL	4.7 mL	4.7 mL	4.7 mL	4.7 mL
Volume of KMnO ₄	4.1 mL	3.8 mL	3.5 mL	3.3 mL	3.0 mL	2.8 mL	2.7 mL	2.7 mL	2.7 mL

Ternary Complexes of Cu (II), Ni (II), Co (II) and La (III) Ions with 2-[(Pyridin-2-Ylmethylidene) Amino] Phenol and Heterocyclic Nitrogen Base

(x)			mL	mL		mL		mL	mL
Volume of H ₂ O ₂ decomposed (a-x)	0.6 mL	0.9 mL	1.2 mL	1.4 mL	1.7 mL	1.9 mL	2.0 mL	2.0 mL	2.0 mL
% of H ₂ O ₂ decomposed(ax)/(a)	12.7	19.1	25.5	29.7	36.1	40.4	42.5	42.5	42.5

Table9. Effect of time on decomposition of H₂O₂ at constant concentration of H₂O₂ (0.15 N) and Co(II) complex (6.8x10⁻³ mmol) at 25 °C.

	Time (Minutes)								
	30	60	90	120	150	180	210	240	270
Baseline KMnO ₄ (a)	4.3 mL	4.3 mL	4.3 mL	4.3 mL	4.3 mL	4.3 mL	4.3 mL	4.3 mL	4.3 mL
Volume of KMnO ₄ (x)	3.5 mL	3.1 mL	2.6 mL	2.2 mL	1.8 mL	1.5 mL	1.3 mL	1.2 mL	1.2 mL
Volume of H ₂ O ₂ decomposed (a-x)	0.8 mL	1.2 mL	1.7 mL	2.1 mL	2.5 mL	2.8 mL	3.0 mL	3.1 mL	3.1 mL
% of H ₂ O ₂ decomposed(ax)/(a)	18.6	27.9	39.5	48.8	58.1	65.1	70	72	72

Table10. Effect of time on decomposition of H₂O₂ at constant concentration of H₂O₂ (0.15 N) and Ni(II) complex (9.0x10⁻³ mmol) at 25 °C.

	Time (Minutes)								
	30	60	90	120	150	180	210	240	270
Baseline KMnO ₄ (a)	4.7 mL	4.7 mL	4.7 mL	4.7 mL	4.7 mL	4.7 mL	4.7 mL	4.7 mL	4.7 mL
volume of KMnO ₄ (x)	4.1 mL	3.9 mL	3.6 mL	3.1 mL	2.8 mL	2.6 mL	2.2 mL	2.2 mL	2.2 mL
Volume of H ₂ O ₂ decomposed (a-x)	0.6 mL	0.8 mL	1.1 mL	1.6 mL	1.9 mL	2.1 mL	3.0 mL	3.1 mL	3.1 mL
% of H ₂ O ₂ decomposed (a-x)/(a)	12.7	17	23.4	34	40.4	44.6	46.8	46.8	46.8

Table11. Effect of time on decomposition of H₂O₂ at constant concentration of H₂O₂ (0.15 N) and La(III) complex (6.4x10⁻³ mmol) at 25 °C.

	Time (Minutes)								
	30	60	90	120	150	180	210	240	270
Baseline KMnO ₄ (a)	4.8 mL	4.8 mL	4.8 mL	4.8 mL	4.8 mL	4.8 mL	4.8 mL	4.8 mL	4.8 mL
volume of KMnO ₄ (x)	4.3 mL	3.9 mL	3.4 mL	3.0 mL	2.6 mL	2.3 mL	2.1 mL	1.9 mL	1.8 mL
Volume of H ₂ O ₂ decomposed (a-x)	0.5 mL	0.9 mL	1.4 mL	1.8 mL	2.2 mL	2.5 mL	2.7 mL	2.9 mL	3.0 mL
% of H ₂ O ₂ decomposed(ax)/(a)	10.4	18.7	29.1	37.7	45.8	52	56.2	60.4	62.5

Table12. Biological activities of ligand (HL) and mixed ligand complexes

Compound	Diameter of inhibition zone (mm)	
	Escherichia coli (G-)	Staphylococcus Aureus (G+)
HL	16	13
[Cu(HL)(2-AP)Cl ₂].H ₂ O	16	18
[Co(HL)(2-AP)Cl ₂].H ₂ O	17	16
[Ni(HL)(2-AP)Cl ₂].H ₂ O	13	14
[La(HL)(2-AP)(NO ₃) ₂].NO ₃	11	15
Tetracycline Antibacterial agent	32	30

4. CONCLUSION

The mixed ligand complexes are formed in the 1:1:1 ratio as found from the elemental analyses and found to have the formulae [M(HL)(2-AP)Cl₂].H₂O and [La(HL)(2-AP)(NO₃)₂].NO₃ where M= Cu(II),

Ni(II) and Co(II) ions, 2-AP = 2-aminopyridine and HL= 2-[(pyridin-2-ylmethylidene)amino]phenol. The molar conductance data reveal that the chelates are non-electrolytes except La(III) complex. The thermal complexes stability investigations enable to evaluate the assumed position of water molecules in the outer or inner sphere of the coordination, to know the mechanism of complex decomposition. The activation thermodynamic parameters, such as, E^* , H^* , S^* and G^* are calculated from the TG curves and discussed. The catalytic activities of the complexes towards hydrogen peroxide decomposition reaction were investigated. The biological activity studies show the possibility to use some of the synthesized compounds as antibacterial agents.

REFERENCES

- [1] Scott, N.M., Schareina, T., Tok, O., Kempe, R., Eur. J. Inorg. Chem. 2004 (2004) 3297.
- [2] Poola, B., Choung, W., Nantz, M.H., Tetrahedron 64 (2008) 10798.
- [3] Yalcin, B., Fatullayeva, P.A., Buyukgungor, O., Kosar, B., Tascioglu, S., Israfilov, A.I., Ibayev, Z.D., Medjidov, A.A., Aydın, A., Polyhedron 26 (2007) 3301.
- [4] Yenikaya, C., Poyraz, M., Sarı, M., Demirci, F., İlkimen, H., Büyükgüngör, O., Polyhedron 28 (2009) 3526.
- [5] Amr, A.G., Mohamed, A.M., Mohamed, S.F., Abdel-Hafez, N.A., Hammam, A. Bioorg. Med. Chem., 14 (2006) 5481.
- [6] Zhuravel, I.O., Kovalenko, S.M., Ivachtchenko, A.V., Balakin, K.V., Kazmirchuk, V., Bioorg. Med. Chem. Lett., 5 (2005) 5483.
- [7] Goel, A., Ram, V.J., Tetrahedron 65 (2009) 7865.
- [8] Al-Hashimy, N.A., Hussein, Y.A., Spectrochim. Acta A 75 (2010) 198.
- [9] Travnicek, Z., Mikulík, J., Cajan, M., Zboril, R., Popa, I., Bioorg Med Chem 16 (2008) 8719.
- [10] McKee, M.L., Kerwin, S.M., Bioorg Med Chem 16 (2008) 1775.
- [11] Khoo, T.J., Break, M.K.b., Crouse, K.A., Tahir, M.I.M., Ali, A.M., Cowley, A.R., Watkin, D.J., Tarafder, M.T.H., InorganicaChimicaActa 413 (2014) 68.
- [12] Ali, O.A.M., El-Medani, S.M., Ahmed, D.A., Nassar, D.A., Journal of Molecular Structure 1074 (2014) 713.
- [13] La Durantaye, L.D., McCormick, T., Jia, W.L., Wang, S., Dalton Trans. (2006) 5675.
- [14] Lin, H.C., Huang, C.C., Shi, C.H., Liao, Y.H., Chen, C.C., Lin, Y.C., Liu, Y.H., Dalton Trans. (2007) 781.
- [15] Basak, S., Sen, S., Banerjee, S., Mitra, S., Rosair, G., Rodriguez, M.T.G., polyhedron 26 (2007) 5104.
- [16] Shebl, M., Spectrochim. Acta (A) 117 (2014) 127.
- [17] Gomathi, V., Selvameena, R., International Journal of Scientific Research 2 (2013) 24.
- [18] Gupta, K.C., Abdulkadir, H.K., J. of Macromolecular Sci. A 45 (2008) 53.
- [19] Demetgul, C., Carbohydrate Polymers 89 (2012) 354.
- [20] Hosny, N.M., Trans. Met. Chem., 32 (2007) 117.
- [21] Gudasi, K.B., Patil, S.A., Vadavi, R.S., Shenoy, R.V., Patil, M.S., J. Transition Met. Chem., 30 (2005) 726.
- [22] Shebl, M., Spectrochim. Acta A 70 (2008) 850.
- [23] Taha, Z.A., Ajlouni, A.M., Al Momani, W., J. of Luminescence 132 (2012) 2832.
- [24] Jadhav, S.M., Shelke, V.A., Shankarwar, S.G., Munde, A.S., Chandrashekar, T.K., J. Saudi Chem. Soc. (2011) doi:10.1016.
- [25] Naik, K.H.K., Selvaraj, S., Naik, N., Spectrochim. Acta A 131(2014) 599.
- [26] Abd El-Wahab, Z.H., J.Coord.Chem. 61 (2008)3284.
- [27] Reiss, A., Florea, S., Caproiu, T., Stanica, N., Turk J. Chem. 33 (2009) 775.
- [28] Lever, A.B.P., Electronic Spectra of d^n Ions in Inorganic Electronic Spectroscopy, second ed., Elsevier, Amsterdam, The Netherlands, 1984.
- [29] Mohamed, G.G., Omar, M.M., Hindy, A.M.M., J. Spectrochim. Acta A 62 (2005) 1140.
- [30] Mohamed, G.G., Abd El-Wahab, Z.H., J. Spectrochim. Acta A 61 (2005) 1059.
- [31] Abd El-Wahab, Z.H., Mashaly, M.M., Salman, A.A., El-Shetary, B.A., Faheim, A.A., J. Spectrochim. Acta (A) 60 (2004) 2861.
- [32] Ali, O.A.M., Spectrochim. Acta (A) 121 (2014) 188.
- [33] Majumder, A., Rosair, G.M., Mallick, A., Chattopadhyay, N., Mitra, S., J. Polyhedron 25 (2006) 1753.
- [34] Coats, A.W., Redfern, J.P., Nature 20 (1964) 68.
- [35] Taakeyama, T., Quinn, F., Thermal Analysis, Fundamentals and Applications to Polymer Science, John Wiley and Sons, Chichester, 1994.

- [36] Frost, A.A., Pearson, R.G., Kinetics and Mechanisms, Wiley, New York, 1961.
- [37] Hosny, N.M., Trans. Met. Chem. 32 (2007) 117.
- [38] Gupta, K.C., Abdulkadir, H.K., J. of Macromolecular Sci. A 45 (2007) 53.
- [39] Demetgul, C., Carbohydrate Polymers 89 (2012) 354.
- [40] Lousada, C.M., Jonsson, M., J. Phys. Chem. 114 (2010) 11202.
- [41] Zigah, D., Lopez, J.R., Bard, A., J. Phys. Chem. 14 (2012) 12764.
- [42] Chithra, P.G., Nisha, J.T., Beena, B., Indian Journal of Chemical Technology 16 (2009) 188.
- [43] Dharmaraj, N., Viswanathamurthi, P., Nataragan, K., J. Transition Met. Chem. 26 (2001) 105.
- [44] Garg, R., Fahmi, N., Singh, R.V., Russian Journal of Coordination Chemistry 33 (2007) 761.

Citation: Omyma A. M. Ali, et.al, " Ternary Complexes of Cu(II), Ni(II), Co(II) And La(III) Ions with 2-[(Pyridin-2- Ylmethylidene) Amino]Phenol and Heterocyclic Nitrogen Base", International Journal of Advanced Research in Chemical Science, vol. 6, no. 8, p. 21-32, 2019. DOI: <http://dx.doi.org/10.20431/2349-0403.0608004>

Copyright: © 2019 Authors. This is an open-access article distributed under the terms of the Creative Commons Attribution License, which permits unrestricted use, distribution, and reproduction in any medium, provided the original author and source are credited.